Available online at www.sciencedirect.com

SCIENCE DIRECT®

Journal of Organometallic Chemistry 691 (2006) 1927–1933

Journal of Organometallic Chemistry

www.elsevier.com/locate/jorganchem

Quantum chemistry studies on the Ru–M interactions and the ^{31}P NMR in $[Ru(CO)_3(Ph_2Ppy)_2(MCl_2)]$ (M = Zn, Cd, Hg)

Xuan Xu [a,b], Liang Fang [b], Zhao-Xing Chen [b], Guo-Chun Yang [a], Shi-Ling Sun [a], Zhong-Min Su [a,*]

[a] *Institute of Functional Material Chemistry, Faculty of Chemistry, Northeast Normal University, No. 5268 Renmin Street, Changchun 130024, Jilin Province, China*

[b] *School of Chemistry and Environment, South China Normal University, Guangzhou 510631, Guangdong Province, China*

Received 15 November 2005; received in revised form 30 December 2005; accepted 6 January 2006

Abstract

To study the Ru–M interactions and their effects on ^{31}P NMR, complexes $[Ru(CO)_3(Ph_2Ppy)_2]$ (py = pyridine) (**1**) and $[Ru(CO)_3(Ph_2Ppy)_2MCl_2]$ (M = Zn, **2**; Cd, **3**; Hg, **4**) were calculated by density functional theory (DFT) PBE0 method. Moreover, the PBE0-GIAO method was employed to calculate the ^{31}P chemical shifts in complexes. The calculated ^{31}P chemical shifts in **1**–**3** follow **2** > **3** > **1** which are consistent to experimental results, proving that PBE0-GIAO method adopted in this study is reasonable. This method is employed to predict the ^{31}P chemical shift in designed complex **4**. Compared with **1**, the ^{31}P chemical shifts in **2**–**4** vary resulting from adjacent Ru–M interactions. The $Ru \rightarrow M$ or $Ru \leftarrow M$ charge-transfer interactions in **2**–**4** are revealed by second-order perturbation theory. The strength order of $Ru \rightarrow M$ interactions is the same as that of the $P\text{–}Ru \rightarrow M$ delocalization with Zn > Cd > Hg, which coincides with the order of ^{31}P NMR chemical shifts. The interaction of $Ru \rightarrow M$, corresponding to the delocalization from 4d orbital of Ru to s valence orbital of M^{2+}, results in the delocalization of $P\text{–}Ru \rightarrow M$, which decreases the electron density of P nucleus and causes the downfield ^{31}P chemical shifts. Except **2**, the back-donation effect of $Ru \leftarrow M$, arising from the delocalization from s valence orbital of M^{2+} to the valence orbital of Ru, is against the $P\text{–}Ru \rightarrow M$ delocalization and results in the upfield ^{31}P chemical shifts in **4**. Meanwhile, the binding energies indicate that complex **4** is stable and can be synthesized experimentally. However, as complex $[Ru(CO)_3(Ph_2Ppy)_2HgCl]^+$ **5** is more stable than **4**, the reaction of **1** with $HgCl_2$ only gave **5** experimentally.

Keywords: $[Ru(CO)_3(Ph_2Ppy)_2(MCl_2)]$ (M = Zn, Cd, Hg); DFT; GIAO; Metal–metal interaction; ^{31}P NMR

---

1. Introduction

Over the past two decades, heterometallic complexes containing metal–metal bond have been extensively studied due to their unique structures and properties including catalysis [1–6] and spectroscopy [2,5,7–9]. Much interest is focused on the study of polydentate ligands with main-group donors that are able to form various polynuclear complexes, such as 2-(diphenylphosphino)pyridine (Ph_2Ppy) [2,3,5], 2,6-bis(diphenylphosphino)pyridine [2,5], bis(dimethylphosphino)methane(dmpm) [10], bis(diphenylphosphino)methane(dppm) [2,4].

Ph_2Ppy is an unsymmetrical and neutral bidentate ligand with a nitrogen donor atom and a phosphorus atom that can connect two identical or different metal centers. It is also a rigid short-bite ligand because of the presence of the pyridyl ring. As a result, it has small flexibility and can be used to stabilize binuclear complexes, especially heterobinuclear ones, by forming a metal–metal bond and acting as a bridging ligand [7]. The heterobinuclear complexes generally contain a donor–acceptor $M \rightarrow M'$ bond between an electron-rich metal M and a high oxidation-state metal M'^{n+}. Since the coordination

---

[*] Corresponding author. Fax: +86 431 5684009.
E-mail address: zmsu@nenu.edu.cn (Z.-M. Su).

0022-328X/$ - see front matter © 2006 Elsevier B.V. All rights reserved.
doi:10.1016/j.jorganchem.2006.01.051

chemistry of Ph_2Ppy was first developed by Balch et al. [11–13], a lot of studies have been done by several groups. For example, Cotton et al. [14], Faraone et al. [15] and Zhang et al. [16,17,7] have synthesized various novel binuclear complexes involving almost all metal atoms in VIB, VIIB, VIIIB, IB, IIB groups such as palladium, platinum, ruthenium, rhodium, iridium, silver, gold, copper, rhenium, molybdenum, etc. To our knowledge, there has been no theoretical study on the complexes of Ph_2Ppy reported.

Experimentally, Che and Zhang [16] got heterometallic complexes $[Ru(CO)_3(Ph_2Ppy)_2ZnCl_2]$ (**2**) and $[Ru(CO)_3(Ph_2Ppy)_2CdCl_2]$ (**3**) by complex $[Ru(CO)_3(Ph_2Ppy)_2]$ (**1**) with Lewis acids such as $ZnCl_2$ and $CdCl_2$. Complexes **2** and **3** can be considered as simple $Ru \rightarrow M^{2+}$ donor–acceptor bonding adducts via infrared spectra and X-ray crystallography. It was also shown that the strength of $Ru \rightarrow M$ bonding interaction follows the order as $\mathbf{3} \approx \mathbf{2}$. Although Hg is an element of IIB group as well as Zn and Cd, the reaction of **1** with $HgCl_2$ readily afforded $[Ru(CO)_3(Ph_2Ppy)_2(HgCl)]^+$ (**5**) but did not get $[Ru(CO)_3(Ph_2Ppy)_2HgCl_2]$ (**4**). Is the complex **4** stable? Meanwhile, Che and Zhang [16] also found that there are downfield ^{31}P NMR chemical shifts in **2** and **3** contrasted to mononuclear complex **1**. It is not known whether the Ru–M interactions affect the ^{31}P NMR and how the Ru–M interactions affect the ^{31}P NMR. In the present study, the stability of **4** and **5**, the nature of Ru–M interactions and their effects on ^{31}P NMR chemical shifts in binuclear complexes were investigated with theoretical methods.

2. Computational details

Considering that the electron configuration on Ru(0) is $4d^75s^1$, the spin states of complexes, such as singlet, triplet and quintet, were examined with PBE0 [18,19] method and SDD [20] basis sets for Ru, Zn, Cd, Hg atoms, 6-311G* basis set for Cl and P, and 6-31G* basis set for C, N and H atoms. The optimization geometry parameters of singlet states in all complexes were close to crystal data [16], while the distances of Ru–P and Ru–M in triplet and quintet states increased, getting more different from crystal data during the optimizations. Meanwhile, on basis of crystal data of every complex, we calculated the single point energies of singlet, triplet and quintet. It can be seen from Table 1 that the single point energies of singlet states in all complexes were the lowest. The results suggested that the singlet states of all complexes in this study were the most stable on the basis of above calculations. Therefore, the singlet states of all complexes were calculated and analyzed.

Table 1
Computed energies (a.u.) of different spin states of complexes by PBE0 method based on the crystal structures

Complex	Singlet	Triplet	Quintet
1	−2536.9257	−2536.8203	−2536.6793
2	−3684.2172	−3684.1041	−3683.9522
3	−3624.9958	−3624.8764	−3624.7200
5[a]	−3150.4256	−3150.2855	−3150.1303

[a] Cation complex $[Ru(CO)_3(Ph_2Ppy)_2HgCl]^+$ were employed to analyze the stability contrasted to **4**.

The efficiency of the functional and basis sets were considered to describe the geometries of the complexes **1**–**4**. The B3LYP functional and LANL2DZ basis sets, which were usually employed to calculate the geometries and electronic structures in many complexes, were taken as a reference point. Molecular geometry of **2** was optimized at the B3LYP [21] and PBE0 level. Meanwhile, the 16, 20, 20 and 20 valence electron LANL2DZ [22] and SDD basis sets for Ru, Zn, Cd, Hg atoms, respectively, 6-311G* basis set for Cl and P, and 6-31G* basis set for C, N and H atoms were employed. Some calculated geometry parameters of **2** and **3** are listed in Table 2.

The data in Table 2 indicates that the optimized geometries of **2**, performed at both B3LYP and PBE0 levels with LANL2DZ basis sets for metal atoms, reproduces experimental structural parameters well except the Ru–Zn distance which is longer than that in crystal data [16]. But the Ru–Zn distance of 2.769 Å calculated at PBE0 level is closer to the crystal data of 2.660 Å compared to that of 2.813 Å calculated at the B3LYP level. Hence, the PBE0 method gives slightly better Ru–Zn distance in **2**. While comparing the optimized geometries of **2** and **3** performed at PBE0 level with SDD and LANL2DZ basis sets for metal atoms, the larger basis set SDD gives Ru–Zn distance with 2.722 Å and Ru–Cd distance with 2.849 Å, which are closer to the crystal data of 2.660 and 2.771 Å contrast to those calculated at LanL2DZ basis set. Hence, structural parameters obtained by the PBE0 method with SDD basis set are closer to experimental values. Therefore, all the results presented in this study were obtained at the PBE0 levels of DFT theory and SDD basis sets for metal atoms with the GAUSSIAN 03 package [23]. A counterpoise

Table 2
Optimized geometrical parameters in complexes **2** and **3**

Bond length (Å)	$[Ru(CO)_3(Ph_2Ppy)_2ZnCl_2]$ (**2**)				$[Ru(CO)_3(Ph_2Ppy)_2CdCl_2]$ (**3**)		
	Exp.	B3LYP/ LANL2DZ	PBE0/LANL2DZ	PBE0/SDD	Exp.	PBE0/LANL2DZ	PBE0/SDD
Ru–M	2.660	2.813	2.769	2.722	2.771	2.927	2.849
P–Ru	2.344	2.417	2.368	2.354	2.361	2.380	2.366
Ru–C(2)	1.913	1.955	1.939	1.914	1.932	1.941	1.909
Ru–C(1)	1.954	1.964	1.948	1.925	1.942	1.941	1.928
M–Cl	2.328	2.374	2.347	2.290	2.454	2.500	2.476
M–N	2.320	2.374	2.332	2.337	2.503	2.491	2.496

correction was carried out for the basis-set superposition error (BSSE) on the interaction energies [24]. The PBE0-GIAO [25–29] method was adopted to calculate the ^{31}P chemical shifts.

3. Results and discussion

3.1. The structures of complexes

The optimized structures of complexes **1**–**5** are presented in Fig. 1. The P_2Ru unit is nearly linear with P(1)–Ru–P(2) angles range from 170.88° to 179.81° in complexes **1**–**4**. Three CO moieties, Ru and M lie on a plane perpendicular to the P_2Ru axis. In complex **1**, the coordination geometry of Ru exhibits a trigonal-bipyrimidal configuration. However, **2**–**4** show a distorted octahedral geometry about the Ru atom, and M is a trigonal bipyramid (M = Zn, Cd, Hg). The Ru–Hg distance (2.774 Å) in designed complex **4** is shorter than Ru–Cd distance (2.849 Å) in **3** and close to Ru–Zn distance (2.722 Å) in **2**. As contrasted with the sum of covalent radii of Ru and M, this shorter Ru–Hg distance indicates the stronger Ru–Hg interaction than Ru–Cd and Ru–Zn.

3.2. The stability and Ru–M interactions

To depict the stabilities of **2**–**4**, the binding energies Δ*E* between $[Ru(CO)_3(Ph_2Ppy)_2]$ and MCl_2 were calculated with Counterpoise (CP) corrections for basis-set superposition errors (BSSE) according to Eq. (1):

$$\underset{ab}{[Ru(CO)_3(Ph_2Ppy)_2MCl_2]} = \underset{a}{[Ru(CO)_3(Ph_2Ppy)_2]} + \underset{b}{MCl_2}$$
$$\Delta E = (E_T^{a} + E_T^{b}) - E_T^{ab} \tag{1}$$

It is obvious that the Δ*E* involves not only Ru–M interaction, but also N–M–N interaction. In order to analyze the strengths of Ru–M bonding interaction, three simplified model complexes $[Ru(CO)_3(Ph_2PH)_2MCl_2]$ (M = Zn, Cd and Hg), which were obtained by replacing the py groups in **2**–**4** with H atoms, were also studied. The interaction energies ΔE_H between $[Ru(CO)_3(Ph_2PH)_2]$ and MCl_2 fragments were then calculated according to Eq. (1) and are showed in Table 3, which represent more exactly the Ru–M bonding interactions. And ∂*E*, the difference between Δ*E* and ΔE_H, denotes the N–M–N interactions of binuclear complexes.

The larger ΔE_H of **4** (61.50 kcal/mol), compared with those of **2** (56.48 kcal/mol) and **3** (55.72 kcal/mol), indicates that the strength order of Ru–M interactions is Ru–Hg(**4**) > Ru–Cd(**3**) ≈ Ru–Zn(**2**). Moreover, the Wiberg bond indices of Ru–M follow the similar order as **4** (0.1794) ≫ **3**(0.1031)**2** ≈ (0.0953) in Table 4.

The ∂*E* values ranging from 11.30 to 30.43 kcal/mol indicate that the N–M–N interactions of binuclear

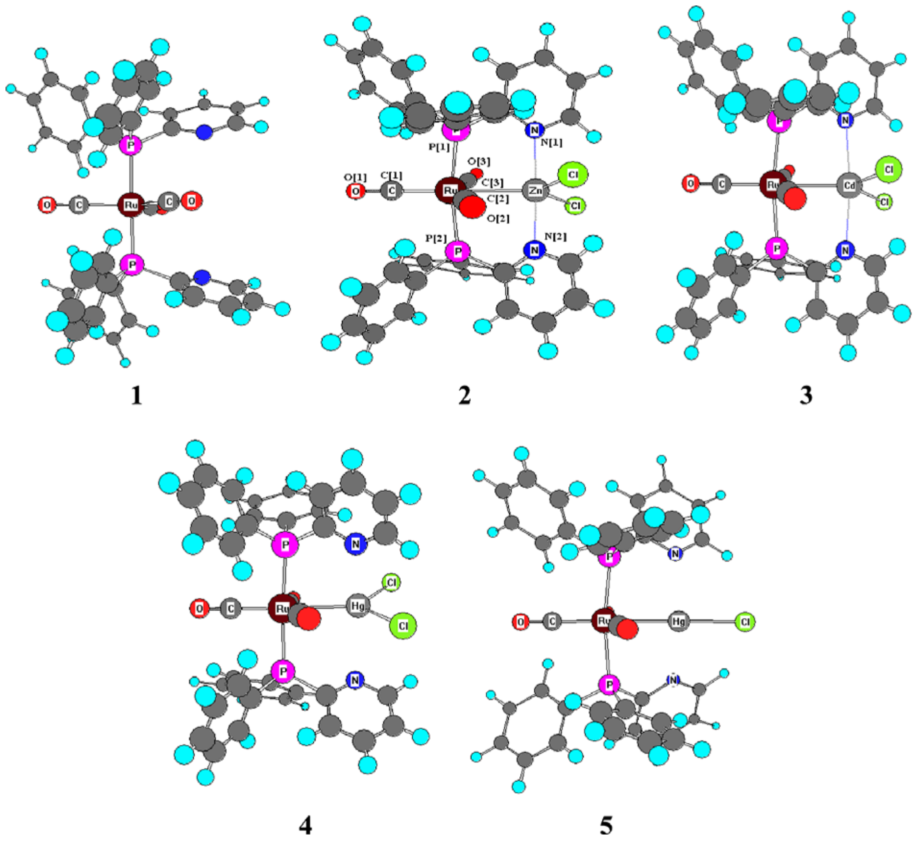

1 **2** **3**

4 **5**

Fig. 1. Optimized structures of complexes **1**–**5** by PBE0 method.

Table 3
Binding energies (kcal/mol) of complexes **2**–**5** with BSSE corrections

	ΔE[a]	ΔE_H[b]	∂E[c]
2	81.76	56.48	25.29
3	86.16	55.72	30.43
4	72.79	61.50	11.30
5[d]	182.10	156.81	25.29

[a] The binding energies between **1** and MCl_2.

[b] Binding energies like ΔE, in which the py groups were instead with H atoms.

[c] The difference between ΔE and ΔE_H.

[d] Cation complex $[Ru(CO)_3(Ph_2Ppy)_2HgCl]^+$ were employed to analyse the stability contrasted to **4**.

complexes are weaker than Ru–M interactions. The binding energies ΔE between $[Ru(CO)_3(Ph_2Ppy)_2]$ and MCl_2, as shown in Table 3, suggest that complexes **1**–**4** are all stable and the stabilities follow the order **2** ≈ **3** > **4**. Although the interaction strength of Ru–Hg is stronger than those of Ru–Zn and Ru–Cd, the N–Hg–N interaction (11.30 kcal/mol) is the weakest for **2**–**4**. Hence, the rather weak N–Hg–N interaction decreases the stability of **4**. To further study the stability of Ru–Hg complex, the structure of cation complex $[Ru(CO)_3(Ph_2Ppy)_2HgCl]^+$ **5** was calculated at the same level as well as **2**–**4**. The binding energies ΔE (182.10 kcal/mol) and ΔE_H (156.81 kcal/mol) of **5** in Table 3 show that cation Ru–Hg complex **5** is more stable than **4**. Therefore, the reaction of **1** with $HgCl_2$ readily afforded **5** but did not get **4**, which favors the conclusion by Zhang et al. [16].

3.3. ^{31}P chemical shifts

Nuclear magnetic resonance (NMR) spectroscopy is becoming an increasingly important tool in studies of intermolecular interactions. In the past decade, it has become possible to carry out theoretical calculations on NMR chemical shifts with increasing accuracy. The application of density functional theory (DFT) has been especially useful for large organic molecules or molecules with transition metal atoms [30–33]. Among methods employed to calculate the NMR parameters such as CSGT, IGLO, GIAO and IGAIM, the GIAO method shows the best basis-set convergence and is employed by most quantum chemistry programs capable of computing nuclear shielding [30,34]. A number of applications have shown that the GIAO-DFT method is capable of reproducing experimental values for chemical shifts of transition metal complexes. The calculated deviations of the NMR shielding in compounds containing heavy elements are usually increased compared with general molecules. For example, Ruiz-Morales and Ziegler [35] calculated the ^{31}P chemical shifts of complexes containing Cr or Mo atom and achieved results with deviations of 10–20 ppm. The 13–22 ppm deviations of ^{31}P chemical shifts were also calculated by Eichele et al. [36] in the complexes containing Ru atom.

Table 4
The NBO Wiberg bond indices of complexes **2**–**4**

Complex	Ru–M	M–N
2	0.0953	0.0624
3	0.1031	0.0622
4	0.1794	0.0420

Phosphorus chemical shielding σ in **1**–**3** and reference H_3PO_4 were carried out by PBE0-GIAO method in this paper. The calculated ^{31}P chemical shielding in H_3PO_4 is 306.82 ppm which is close to 315.5 ppm calculated by Ruiz-Morales and Ziegler using DFT(BP-LDA)-GIAO method [35]. The ^{31}P chemical shifts (δ) relative to the reference H_3PO_4 can be given by $\delta = \sigma_{H_3PO_4} - \sigma_{\text{complex}}$. As seen in Table 5, the calculated ^{31}P chemical shifts (δ_{cal}) in **1**–**3** are in good agreement with experimental values [16]. The largest deviation is only 10 ppm which is much less than that calculated by Ruiz-Morales and Ziegler [35] and Eichele et al. [36]. In addition, the order of calculated ^{31}P chemical shifts coincides with the experiment results as **2** > **3** > **1** [16]. Therefore, PBE0-GIAO method adopted in this work is valid and was thus employed to predict the ^{31}P chemical shift in **4** as well. The ^{31}P chemical shift of 52.09 ppm in **4** is comparable with experimental value of 48.70 ppm in similar structure of **5** [16]. Due to the adjacent Ru–M interaction, the ^{31}P chemical shifts in binuclear complexes **2**–**4** are changed contrasted with mononuclear complex (see Table 5). However, it does not mean that, as Ru–M interaction is stronger, there will be larger downfield ^{31}P chemical shifts.

It is known that the deshielding arising from less electron density of phosphorus moves ^{31}P chemical shifts downfield. Although the NPA charges around P nucleus (see Table 5) in the binuclear complexes are almost unchanged compared with mononuclear complex **1**, the deviation of ^{31}P chemical shifts in **2** and **3** contrasted with **1** can be illustrated by means of the second-order perturbation energy $E(2)$ according to Eq. (2) [37], for a general donor NBO (i) and an acceptor NBO (j):

$$E(2) = E_{ij} = q_i \frac{F(i,j)^2}{\varepsilon_j - \varepsilon_i} \tag{2}$$

where q_i is the donor orbital occupancy, ε_i and ε_j are diagonal elements (orbital energies), and $F(i,j)$ is the off-diagonal element in NBO Fock matrix. The second-order perturbative stabilization energy $E(2)$ has been proved efficient in illustrating the relationship between the donor–acceptor interactions in two NBOs' of adjacent atoms

Table 5
The calculated ^{31}P NMR chemical shift and NPA charge of P atom (Q_P) for complexes **1**–**4**

Complex	δ_{Pexp}	δ_{Pcal}	Q_P
1	50.09	60.70	1.187
2	61.20	67.63	1.182
3	59.40	66.00	1.174
4		52.09	1.191

or bonds and NMR chemical shifts [38–40]. As can be seen from Table 6 that the deshielding for P nucleus in complex **2** is caused by the delocalization of the P–Ru occupied σ bonding orbital into the acceptor 4s orbital of Zn(II) through the Ru → Zn interaction, with $E(2)$ amounting to 28.56 kcal/mol. This delocalization from P–Ru to Zn can also be observed in Fig. 2. As a result, there is a downfield ^{31}P chemical shift in **2** contrasted with **1**. Through the Ru → Cd interaction, the similar deshielding for P nucleus in **3** is derived of the σ(P–Ru) → 5s(Cd) and σ^*(P–Ru) → 5s(Cd) delocalization and $E(2)$ amounts to 1.81 and 17.76 kcal/mol, respectively. The total delocalized effects from P–Ru to Cd are a little less than that from P–Ru to Zn. Therefore, there is slightly less downfield ^{31}P chemical shift in **3** than that of **2**. However in **4**, there are σ(P–Ru) → 6s(Hg) and 6s(Hg) → σ^*(P–Ru) delocalizations with 17.51 and 28.59 kcal/mol, respectively. In view of the stronger 6s(Hg) → σ^*(P–Ru) delocalization that shields P nucleus, the upfield ^{31}P chemical shift in **4** is calculated compared with **1**.

As the deshielding on P nucleus is derived from the delocalized effect of P–Ru → M through the Ru → M interaction, the nature of Ru–M interactions should be studied. The detailed information on the Ru–M (M = Zn, Cd) charge-transfer interactions can be obtained through NBO analyses by means of the second-order perturbation energy $E(2)$, which has already succeeded in illustrating the weak bonding interaction [41–44]. For example, Koch et al. estimated the stabilization energies $E(2)$ of Ni–Ni interactions at the range of 156–252 kJ/mol (37.3–60.3 kcal/mol) in a series of complexes [41].

As shown in Table 7 for complex **3**, two types of Ru–Cd charge-transfer interactions were revealed by second-order perturbation energy $E(2)$. The first one is Ru → Cd charge-transfer interaction corresponding to the delocalization from the occupied lone-pair 4d orbital on Ru(0) atom into the acceptor 5s orbital on Cd(II) atom with 27.08 kcal/mol second-order perturbation energy $E(2)$. This Ru → Cd interaction pulls the charges on P–Ru bonds to Cd atom, which decreases the electron density on P nucleus and causes the downfield ^{31}P NMR chemical shifts. The second one is an additional back-donation Ru ← Cd effect deriving from the delocalization of 5s orbital on Cd(II) into the $5s^{1}4d^{0.11}$ hybrid on Ru(0) atom amounting to 77.61 kcal/mol second-order perturbation energy, which is to a certain extent against the P–Ru → Cd delocalization. However, the $E(2)$ indicates that there is only

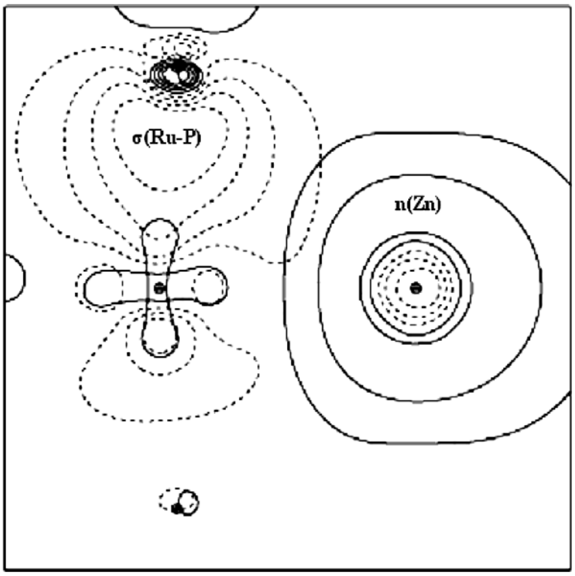

Fig. 2. Contour plots of the overlap of NBOs: Ru–P σ bonding orbital and Zn anti-lone-pair orbital (4s) in complex **2**.

Ru → Zn charge-transfer interaction in **2** corresponding to 4d (Ru) → 4s(Zn^{2+}) delocalization. The Ru → Zn interaction with 49.73 kcal/mol second-order perturbation energy is stronger than Ru → Cd interaction, which resulted in the stronger P–Ru → Zn delocalization and larger downfield ^{31}P chemical shifts in **2**. Since the attraction by nucleus for 4s electron on Zn(II) atom is stronger than that for 5s electron on Cd(II), there is no Ru ← Zn interaction. Similarly to **3**, there are two types of interactions in **4**, Ru → Hg and Ru ← Hg. However, the interaction of Ru → Hg is much weaker than those of Ru → Cd and Ru → Zn, while the interaction of Ru ← Hg (C–Ru ← Hg, P–Ru ← Hg) is much stronger than that of Ru ← Cd and Ru → Hg, the later in particular. As a result, there is a upfield ^{31}P chemical shifts in **4** compared to **1**.

Overall, the strength order of Ru → M (M = Zn, Cd, Hg) interactions in **2**–**4** is the same as that of the P–Ru → M delocalization with Zn > Cd > Hg, which also coincides with the order of ^{31}P chemical shifts. The charge on P–Ru bonds was pulled to M(II) atom owing to the Ru → M interactions, which decreases the electron density of P nucleus and causes downfield ^{31}P chemical shifts. However, the P–Ru ← M delocalization caused by Ru ← M interaction results in upfield ^{31}P chemical shifts to a certain extent.

Table 6
Second-order perturbation energy $E(2)$ (kcal/mol) of donor–acceptor P–Ru–M interactions in the NBO basis

Complex	Occupancy	Donor NBOs	Occupancy	Acceptor NBOs	$E(2)$
2	1.82	$\sigma_{\mathrm{Ru-P}}$	0.54	n (4s 99.87%, Zn)	28.56
3	1.91	$\sigma_{\mathrm{Ru-P}}$	0.57	n (5s 99.86%, Cd)	1.81
	0.77	$\sigma^*_{\mathrm{Ru-P}}$	0.57	n (5s 99.86%, Cd)	17.76
4	1.84	$\sigma_{\mathrm{Ru-P}}$	0.87	n (6s 99.09%, Hg)	17.51
	0.87	n (6s 99.09%, Hg)	0.56	$\sigma^*_{\mathrm{Ru-P}}$	28.59

'n' denotes the lone pair electron orbital.

Table 7
The second-order perturbation energy $E(2)$ (kcal/mol) of donor–acceptor interactions about Ru–M in the NBO analysis

Complex	Occupancy	Donor NBOs	Occupancy	Acceptor NBOs	$E(2)$
2	1.69	n (4d 97.65%, Ru)	0.54	n (4s 99.87%, Zn)	49.73
3	1.53	n (4d 99.99%, Ru)	0.57	n (5s 99.86%, Cd)	27.08
	0.57	n (5s 99.86%, Cd)	0.53	n (sd$^{0.11}$, Ru)	77.61
4	1.70	n (4d 99.89%, Ru)	0.87	n (6s 99.09%, Hg)	1.02
	0.87	n (6s 99.09%, Hg)	0.84	$\sigma^*_{\text{Ru–C(1)}}$	141.07
	0.87	n (6s 99.09%, Hg)	0.62	$\sigma^*_{\text{Ru–C(2)}}$	25.84
	1.93	$\sigma_{\text{Ru–C(1)}}$	0.87	n (6s 99.09%, Hg)	4.56
	1.92	$\sigma_{\text{Ru–C(2)}}$	0.87	n (6s 99.09%, Hg)	10.56

4. Conclusion

This study attempted to calculate the structures of complexes **1**–**4** by using PBE0 method, with the purpose of elucidate the stabilities, the nature of Ru–M interactions and the effects of Ru–M interactions on ^{31}P chemical shifts. The following conclusions can be drawn.

The stability follows **2**(Zn) $\approx$ **3**(Cd) > **4**(Hg) due to the rather weak N–Hg–N interaction in **4**, while the order of Ru–M interaction strength is **2**(Ru–Zn) $\approx$ **3**(Ru–Cd) < **4**(Ru–Hg). Hence, **4** is theoretically stable and experimental synthesis is in turn possible. However, **5** is more stable than **4**. As a result, the reaction of **1** with $HgCl_2$ readily afforded **5** but did not give **4**.

The calculated ^{31}P chemical shifts in **1**–**3** follows the order **2** > **3** > **1** which are consistent to experimental results. Therefore, the PBE0-GIAO method adopted in this study proved to be valid and was employed to predict the ^{31}P chemical shift with 52.09 ppm in designed complex **4**.

The ^{31}P chemical shifts in **2**–**4** are changed as a result of the adjacent Ru–M interaction contrasted with **1**. The Ru → M and Ru ← M charge-transfer interactions in **2**–**4** were revealed by second-order perturbation energy $E(2)$. The strength order of Ru → M interactions is the same as that of P–Ru → M delocalization with Zn > Cd > Hg, which coincides with that of ^{31}P chemical shifts. The Ru → M interactions, corresponding to the delocalization from 4d orbital of Ru to s valence orbital of M^{2+}, result in the delocalization of P–Ru → M which decreases the electron density of P nucleus and causes the downfield ^{31}P chemical shifts. Except for **2**, the Ru ← M back-donation effect, arising from the delocalization from s valence orbital of M^{2+} to the valence orbital of Ru, is against the P–Ru → M delocalization and results in the upfield ^{31}P chemical shifts in **4**.

Acknowledgements

Authors acknowledge the financial support from the National Natural Science Foundation of China (Project Nos. 20373009 and 20162005).

References

[1] C. Archambault, R. Bender, P. Braunstein, Y. Dusausoy, J. Chem. Soc., Dalton Trans. (2002) 4084.

[2] P. Espinet, K. Soulantica, Coord. Chem. Rev. 93 (1999) 499.

[3] H. Ishii, M. Goyal, M. Ueda, K. Takeuchi, M. Asai, J. Mol. Catal. A 148 (1999) 289.

[4] M.M. Dell'Anna, S.J. Trepanier, R. McDonald, M. Cowie, Organometallics 20 (2001) 88–99.

[5] Z.Z. Zhang, H. Cheng, Coord. Chem. Rev. 147 (1996) 1.

[6] LA. Mendez, J. Jimenez, E. Cerrada, F. Mohr, M. Laguna, J. Am. Chem. Soc. 127 (2005) 852.

[7] S.M. Kuang, F. Xue, Z.Z. Zhang, W.M. Xue, C.M. Che, T.C.W. Mak, J. Chem. Soc., Dalton Trans. (1997) 3409.

[8] L. Hao, M.A. Mansour, R.J. Lachicotte, H.J. Gysling, R. Eisenberg, Inorg. Chem. 39 (2000) 5520.

[9] B.H. Xia, H.X. Zhang, C.M. Che, K.H. Leung, D.L. Phillips, N. Zhu, Z.Y. Zhou, J. Am. Chem. Soc. 125 (2003) 10362.

[10] B.H. Xia, C.M. Che, D.L. Phillips, Inorg. Chem. 41 (2002) 3866.

[11] J.P. Farr, M.M. Olmstead, A.L. Balch, J. Am. Chem. Soc. 102 (1980) 6654.

[12] J.P. Farr, M.M. Olmstead, F.E. Wood, A.L. Balch, J. Am. Chem. Soc. 105 (1983) 792.

[13] A.L. Balch, H. Hope, F.E. Wood, J. Am. Chem. Soc. 107 (1985) 6936.

[14] T.J. Barder, S.M. Tetrick, R.A. Walton, F.A. Cotton, G.L. Powell, J. Am. Chem. Soc. 105 (1983) 4090.

[15] S. Lo Schiavo, E. Rotondo, G. Bruno, F. Faraone, Organometallics 10 (1991) 1613.

[16] W.H. Chan, Z.Z. Zhang, T.C.W. Mak, C.M. Che, J. Chem. Soc., Dalton Trans. (1998) 803.

[17] S.J. Shieh, D. Li, S.M. Peng, C.M. Che, J. Chem. Soc., Dalton Trans. (1993) 195.

[18] J.P. Perdew, K. Burke, M. Ernzerhof, Phys. Rev. Lett. 78 (1997) 1396.

[19] C. Adamo, V. Barone, J. Chem. Phys. 110 (1999) 6158.

[20] P. Schwerdtfeger, M. Dolg, W.H.E. Schwarz, G.A. Bowmaker, P.D.W. Boyd, J. Chem. Phys. 91 (1989) 1762.

[21] A.D. Becke, J. Chem. Phys. 98 (1993) 5648.

[22] P.J. Hay, W.R. Wadt, J. Chem. Phys. 82 (1985) 299.

[23] M.J. Frisch, G.W. Trucks, H.B. Schlegel, G.E. Scuseria, M.A. Robb, J.R. Cheeseman, J.A. Montgomery Jr., T. Vreven, K.N. Kudin, J.C. Burant, J.M. Millam, S.S. Iyengar, J. Tomasi, V. Barone, B. Mennucci, M. Cossi, G. Scalmani, N. Rega, G.A. Petersson, H. Nakatsuji, M. Hada, M. Ehara, K. Toyota, R. Fukuda, J. Hasegawa, M. Ishida, T. Nakajima, Y. Honda, O. Kitao, H. Nakai, M. Klene, X. Li, J.E. Knox, H.P. Hratchian, J.B. Cross, C. Adamo, J. Jaramillo, R. Gomperts, R.E. Stratmann, O. Yazyev, A.J. Austin, R. Cammi, C. Pomelli, J.W. Ochterski, P.Y. Ayala, K. Morokuma, G.A. Voth, P. Salvador, J.J. Dannenberg, V.G. Zakrzewski, S. Dapprich, A.D. Daniels, M.C. Strain, O. Farkas, D.K. Malick, A.D. Rabuck, K. Raghavachari, J.B. Foresman, J.V. Ortiz, Q. Cui, A.G. Baboul, S. Clifford, J. Cioslowski, B.B. Stefanov, G. Liu, A. Liashenko, P. Piskorz, I. Komaromi, R.L. Martin, D.J. Fox, T. Keith, M.A. Al-Laham, C.Y. Peng, A. Nanayakkara, M. Challacombe, P.M.W. Gill, B. Johnson, W. Chen, M.W. Wong, C. Gonzalez, J.A. Pople, GAUSSIAN 03[CP], Revision B.03, Gaussian Inc., Pittsburgh, PA, 2003.

[24] A. Stützer, P. Bissinger, H. Schmidbaur, Chem. Ber. 125 (1992) 367.

[25] F. London, J. Phys. Radium 8 (1937) 397.

[26] R. Mc Weeny, Phys. Rev. 126 (1962) 1028.

[27] R. Ditchfield, Mol. Phys. 27 (1974) 789.

[28] J.L. Dodds, R. Mc Weeny, A.J. Sadlej, Mol. Phys. 41 (1980) 1419.

[29] K. Wolinski, J.F. Hilton, P. Pulay, J. Am. Chem. Soc. 112 (1990) 8251.

[30] T. Helgaker, M. Jaszundki, K. Ruud, Chem. Rev. 99 (1999) 293.

[31] G. Schreckenbach, T. Ziegler, J. Phys. Chem. 99 (1995) 606.

[32] G. Schreckenbach, T. Ziegler, Int. J. Quantum Chem. 60 (1996) 753.

[33] C. Adamo, V. Barone, Chem. Phys. Lett. 298 (1998) 113.

[34] T. Kupka, G. Pasterna, P. Lodowski, W. Szeja, Magn. Reson. Chem. 37 (1999) 421.

[35] Y. Ruiz-Morales, T. Ziegler, J. Phys. Chem. A 102 (1998) 3970.

[36] K. Eichele, R.E. Wasylishen, J.F. Corrigan, N.J. Taylor, A.J. Carty, K.W. Feindel, G.M. Bernard, J. Am. Chem. Soc. 124 (2002) 1541.

[37] J.E. Carpenter, F.J. Weinhold, Mol. Struct. (Theochem.) 169 (1988) 41.

[38] P. Zhou, Steve C.F. Au-Yeung, X.P. Xu, J. Am. Chem. Soc. 121 (1999) 1030.

[39] M. Iwaoka, H. Komatsu, T. Katsuda, S. Tomoda, J. Am. Chem. Soc. 126 (2004) 5309.

[40] Donald B. DuPre, J. Phys. Chem. A 109 (2005) 622.

[41] J. Koch, I.H. Kryspin, R. Gleiter, T. Klettke, Dirk Walther, Organometallics 18 (1999) 4942.

[42] M.L. DeRider, S.J. Wilkens, M.J. Waddell, L.E. Bretscher, F. Weinhold, R.T. Raines, J.L. Markley, J. Am. Chem. Soc. 124 (2002) 2497.

[43] S.X. Tian, J. Phys. Chem. B 108 (2004) 20388.

[44] H.M.T. Nguyen, M.T. Nguyen, J. Peeters, Th. Zeegers-Huyskens, J. Phys. Chem. A 108 (2004) 11101.